Journal of Low Temperature Physics, Vol. 99, Nos. 5/6, 1995

The Static and Dynamic Properties of Vicinal Surfaces on Helium 4 Crystals

E. Rolley, C. Guthmann, E. Chevalier, and S. Balibar

Laboratoire de Physique Statistique, Ecole Normale Supérieure, 24 rue Lhomond, 75231 Paris Cedex 05, France*

(Received October 25, 1994; revised January 19, 1995)

We have studied melting-freezing waves propagating at low temperature ($40 < T < 500$ mK) on vicinal surfaces of hcp helium 4 crystals, which are tilted by a small angle ϕ with respect to c facets. We have first obtained the experimental evidence of a crossover angle $\phi_c \approx 2.5°$, where the surface properties change from stepped and anisotropic to rough and isotropic. This result confirms our previous prediction[1] that such a crossover should occur at the small angle where the large step width is comparable to the average distance between steps. It also confirms the hypothesis that crystal surfaces are weakly coupled to the lattice in helium. In the $\phi \to 0$ limit, we observed a clear stepped behaviour: the longitudinal component of the surface stiffness vanishes while the transverse component diverges. A quantitative analysis of these two components allowed us to measure the step energy and the interactions between steps. Good agreement is found with the prediction that step interactions result from the combination of elastic and entropic effects. We also found evidence that helium 3 impurities adsorb on the liquid-solid interface and lower the step energy when ordinary helium 4 (130 ppb of ^{3}He) is used instead of an ultrapure sample (0.4 ppb). Furthermore, from the damping of the waves, we could study the dynamics of vicinal surfaces, i.e. their mobility as a function of temperature, angle and frequency. Here too, a crossover is observed from stepped to rough behavior. The dynamics is sensitive to the existence of steps up to higher angles than the stiffness. We show that a true stepped behavior is observed only if two conditions are fulfilled: the distance between steps must be much larger than the step width, and also larger than the mean wavelength of thermal phonons. By changing the frequency, we could finally confirm that the surface mobility increases when the phonon mean free path becomes smaller than the wavelength of the melting-freezing waves. We conclude with some suggestions for further theoretical and experimental studies.

*Associé au CNRS et aux Universités Paris 6 et 7.

0022-2291/95/0600-0851$07.50/0

1. INTRODUCTION

A crystal surface is called "vicinal" if it is slightly tilted with respect to a smooth dense face, in other words if its normal $\vec{n}$ makes a small angle ϕ with some high symmetry direction $\vec{n}_0$. Such a surface is expected to be very anisotropic if it can be considered as a kind of atomic staircase, i.e., a set of terraces separated by steps. Its surface properties are very different in the maximum slope direction and in that perpendicular to it. For a wide variety of applications, it can be interesting to take advantage of this anisotropy: one can try to make various kinds of one or two-dimensional objects or to orient domains of adsorbed layers. It is thus important to understand the properties of vicinal crystal surfaces.

However, as we shall see, the above qualitative description is valid only if the tilt angle ϕ is small enough.[1] In such a case, the surface is called a "stepped" surface because its properties are governed by those of steps: their energy, their width, their density and their interactions. Let us call a the step height ($a = 2.99$ Å) and d the average width of terraces, i.e., the average distance between steps. If the tilt angle ϕ is too large, the distance $d = a/\tan\phi$ is too small for these terraces to be well defined, the staircase disappears and the surface is nearly isotropic. Stepped surfaces are thus expected to exist only in a limited angular domain[1] which depends on the correlation length ξ of terraces, a quantity which can be related to the step width w.[1–5] In this article, we first show that a crossover from anisotropic stepped behavior to isotropic rough behavior[6] can indeed be observed, and that it occurs at an angle which can be estimated according to the above physical argument.

During the last decade, the measurement of the interaction between steps progressively appeared as a real challenge. Indeed these interactions determine not only the equilibrium shape of crystals near facet edges[8] but also the magnitude of step fluctuations, the distribution of terrace widths on vicinal surfaces,[9] and eventually the roughening transition of these vicinal surfaces.[7] Most existing theories predict that neighboring steps should repel each other with a positive interaction energy proportional to $1/d^2$. The physical origin for such a $1/d^2$ repulsion can be elastic (the overlap of strain fields around neighboring steps), entropic (steps do not cross each other since overhangs are unlikely), or dipolar (on metallic surfaces). However, disorder could change this law[10] to $1/d$ and other possible mechanisms have also been proposed.[11,12]

Moreover various types of experiments led to contradictory results. Some authors studied the equilibrium shape of Pb,[13] In[14] or He crystals.[15] A $1/d^2$ repulsion implies that, near the facet edge, the profile equation is $z \approx x^{3/2}$, while a $1/d$ repulsion leads to $z \approx x^2$. However, the exact location

of the facet edge is very difficult, and it is hard to distinguish between the two possible shapes whose observations were both reported.[13–15] Another method was used by Wang *et al.*[16] and Alfonso *et al.*,[17] who measured the width σ of the distribution of terrace sizes on Si surfaces; unfortunately, σ depends only weakly[9] on the nature of interactions ($\sigma \approx d$ for $1/d^2$ and $\sigma \approx d^{3/4}$ for $1/d$ interactions) so that a definite conclusion was hard to draw.[18] Finally, the case of Cu ($11n$) surfaces also seems unclear, since the study of roughening transitions was consistent with a $1/d^2$ repulsion,[7] but attractive interactions were found from STM studies.[19]

It therefore appeared interesting to clarify the problem of step-step interactions by studying helium 4 crystals with more accuracy. Indeed, on helium 4 crystals, step energies and step interactions can be measured from a rather different type of experiment. At low enough temperature, these crystals are able to grow or melt so easily, i.e. with such a small dissipation, that it is possible to propagate melting-freezing waves[20] on their surface. Sometimes also called "crystallization waves", they result from the alternative growth and melting of the crystals. These waves are very similar to ordinary waves at the free surface of a liquid. Indeed, the restoring forces to a flat horizontal surface are the same (gravity and surface tension) and the inertia is similar (growth and melting imply a flow of mass in the liquid since the two densities ρ_c and ρ_L are different). As for ordinary capillary waves, an accurate measurement of the surface tension can thus be made from the study of the dispersion relation. However, the anisotropy of stepped surfaces leads to a large anisotropy of melting-freezing waves, a major difference with liquid surfaces. As a consequence, in the case of melting-freezing waves, the relevant quantity for capillary effects is no longer the surface tension α but the surface stiffness γ, more precisely the stiffness tensor

$$\gamma_{ij} = \alpha + \frac{\partial^2 \alpha}{\partial \phi_i \partial \phi_j} \tag{1}$$

where $\phi_{i,j}$ are angles in some reference frame.

Consider for instance a vicinal surface with a small tilt angle ϕ with respect to a c facet: the surface displays well separated steps. If the wave vector $\vec{q}$ lies perpendicular to the steps, the steps remain straight and the wave induces a local modulation of the step density. The surface stiffness depends on the compressibility of the step system,[4] and its relevant component is

$$\gamma_{\parallel} = \alpha + \frac{\partial^2 \alpha}{\partial \phi^2} = \frac{6\delta}{a^3}\phi \tag{2}$$

In Nozières' notation, $\gamma_{||}$ refers to the projection of the c axis being parallel to the wave vector $\vec{q}$, and Eq. 2 supposes that the interaction per unit length is δ/d^2. From Eq. 2 one finds that the stiffness $\gamma_{||}$ vanishes as the tilt angle ϕ goes to zero. It has the following physical meaning: as the distance d increases, the step interactions vanish and very little energy is spent on bending the surface by moving the steps with respect to one another.

In contrast, if $\vec{q}$ is perpendicular to the projection of the c axis, the wave bends the steps without changing their mutual distance and the restoring force for such a transverse wave is the line tension, i.e., the step free energy β. Assuming cylindrical symmetry around the c axis, the corresponding surface stiffness is now:[4]

$$\gamma_{\perp} = \alpha + \frac{1}{\tan\phi}\frac{\partial\alpha}{\partial\phi} = \frac{\beta}{a\phi} \tag{3}$$

In order to obtain a given interface curvature, more and more bending of steps is needed as ϕ tends to zero, because the step density also vanishes. Step energies and step interactions can thus be measured by studying the propagation of melting-freezing waves. As ϕ tends to zero, Eqs. 2 and 3 predict that $\gamma_{||}$ vanishes while $\gamma_{\perp}$ diverges, so that the wave velocity should be very different along or across steps.

Andreeva *et al.*[21] first tried to check Eq. 2. However, their results triggered further controversies. Indeed, instead of observing a linear vanishing of $\gamma_{||}$, they observed a slight increase, and Andreev concluded that facets do not really exist on helium crystals.[22] At that time, we replied[1] that Andreeva's experiment should be extended to lower temperature and smaller tilt angle where clear evidence of stepped behavior and a reliable measurement of step interactions should be obtained. We predicted that the stepped behavior would appear below the small angle 2.5° only, a consequence of the "weak coupling" which makes the step width rather large on helium crystal surfaces.

We here present a full description of our experiment which is similar to the one by Andreeva *et al.*[21] It was performed at smaller tilt angles and much lower temperature and we found very good agreement with Eqs. 2 and 3. Some of our preliminary results have already been published;[23] they concerned static properties, more precisely the effect on the surface stiffness of the crossover from stepped to rough behavior. Since then, we improved the stability of our crystals and made more precise measurements with an ultrapure helium 4 sample. This allows us to present here a complete description of these surfaces, i.e., not only their static properties but also their dynamic properties.

In Sec. 2, we describe our experimental set up and methods. Section 3 is a full analysis of our stiffness measurements. We first describe the observed crossover from stepped to rough. We then present our measurements of the step energy and explain why they are again consistent with our predictions[1] based on Nozières' hypothesis of a weak coupling of the surface to the crystal lattice. From our measurements of the step interactions as a function of temperature, we then obtain the first experimental evidence for a combination of elastic and entropic repulsion between steps, whose amplitude is found consistent with predictions.[4,9,24,25,26] We also consider the effect of impurities but only briefly, since a longer analysis is published elsewhere.[27]

In Sec. 4, we first present our measurements of the dynamics of vicinal surfaces as a function of temperature and orientation. Andreeva's results[21] already showed that the crossover from rough to stepped behavior happens at a much larger angle for the surface mobility than for the static properties (the surface stiffness). Being more complete, our data allow us to present a full interpretation of this effect. Besides the step width w and the distance d between steps, a third length scale plays a role in the interface dynamics: the mean wavelength λ_{ph} of thermal phonons whose scattering at the interface is responsible for the dissipation. Following Nozières and Uwaha,[28] we show that our results can be understood with the two following arguments:

— the phonon scattering changes from coherent when d is smaller than λ_{ph} to incoherent when d is larger than λ_{ph}.

— a true stepped behavior exists only if d is much larger than λ_{ph} *and* larger than the step width w.

We conclude with a summary of this work and some suggestions for future experiments. Of particular interest would be a measurement of the density and energy of kinks on the steps of helium crystals.

2. EXPERIMENTAL SET UP AND METHODS

2.1. Cryogenics

^{4}He crystals are studied in the temperature range 40–500 mK in an optical dilution cryostat. The dilution unit was purchased from the company Leitec in Leiden (The Netherlands). Thanks to a roots pump (Edwards EH1200), a 800 μmole/s circulation rate can be achieved, which provides a cooling power of 70 μW at 30 mK, at the mixing chamber. Crystals are observed through five windows separated by vacuum and indium sealed on the 300 K, 77 K, 4 K, 0.7 K shields and on the pressure cell

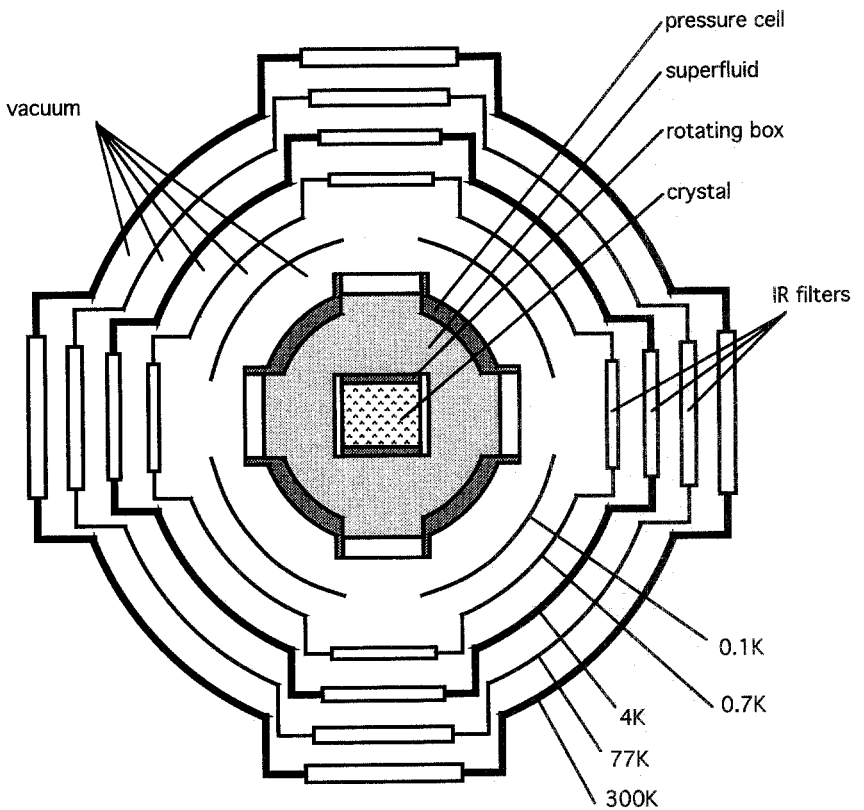

Fig. 1. Schematic cross section of the bottom part of the cryostat, showing the four sets of windows. On the shields at 77 K, 4 K and 0.7 K the windows are coated IR filters.

(Fig. 1). For better mechanical strength and thermal conductivity, the cell windows are made out of sapphire. The other windows are made of coated Pyrex glass so that the transmission coefficient for infrared radiation is less than 1% for wavelengths larger than 0.8 μm.[29] The smallest window has a diameter of 30 mm, so that the observation field is quite large. The cryostat is provided with four series of such windows, allowing direct observation in two perpendicular directions. The total heat losses due to infrared radiation are of the order of 10 μW. The Kapitza resistance between the cell and the mixing chamber being $\approx$2000 K/W at 100 mK, our lowest temperature is 20 mK. The volume of the cell is about 300 cm^3, much larger than the crystal size ($\approx$10 cm^3). The temperature is measured thanks to several Speer carbon resistors in the cell. They had been previously calibrated against the ^{3}He melting curve. The final accuracy of the temperature measurement is 1%.

Special attention has been paid to vibration insulation. The cryostat is fixed on a 2 tons optical bench lying on four active isolators (Melles-Griot 07 OTI 016). The horizontality of the bench is controlled to better than 10^{-5} rad. The pumping line for the mixture involves several bellows and an intermediate section of the line is embedded in the wall of the experimental room.

2.2. Crystal Growth

The first step in the experiment is to grow a high quality single crystal. It is grown at constant pressure by adding ultrapure ^4He[30] through the filling capillary. In order to study solid-liquid interfaces with a crystalline orientation close to the c axis, we need first to nucleate a crystal with the c axis nearly vertical. This is done by using a technique first developed in Moscow.[20] A strong electric field is produced by applying 1000V to a double winding of thin insulated copper wire (0.05 mm diameter), which is located in the upper part of the cell. Due to the difference in permittivity between the solid and the liquid phase, the crystal first nucleates on the wires. Below 1 K, the seed grows like a flat hexagonal prism; when it reaches 3 or 4 mm in size, it falls down to the bottom of the cell, often with the hexagonal facet roughly horizontal. We then partially melt the crystal until its size is of the order of 1 mm^3, and we grow it again very slowly thanks to a regulated flowmeter. At this stage, the speed of the interface is of the order of 0.1 μm/s, and the temperature is lower than 0.1 K.

At such a temperature, the interface is partially faceted and some facets usually touch the walls of the small box where the crystal is grown. These walls are polished in order to avoid the anchoring of facets on irregularities. Indeed, if such an anchoring occurs, the overpressure builds up at the interface until the facet jumps quickly to another position. Such jumps create defects, probably stacking faults. Thanks to the polishing, we could maintain a regular growth with a very small velocity till the crystal reaches its final size (≈ 10 cm^3).

The growth of facets occurs through the motion of steps, which are presumably supplied by a small number of screw dislocations.[31] The typical difference in chemical potential $\Delta\mu_f$ across the facets can be estimated from the radius of curvature R of the rounded parts in between the facets. As these parts are rough, they are close to equilibrium so that the capillary overpressure γ/R compensates the change in pressure δp_L with respect to the equilibrium pressure for a planar interface. This yields: $\Delta\mu_f = \delta p_L(\rho_c - \rho_L)/\rho_c\rho_L = \gamma/R\rho_c$ where ρ_L and ρ_c are the respective densities of the liquid and the solid phases. Here we have assumed thermal equilibrium and neglected the capillary term involving the facet size[4] since this size is much larger during growth than at equilibrium. With $\gamma \approx 0.2$ erg/cm^2 and

$R \approx 1$ mm, we find $\rho_c \Delta\mu \approx 2 \times 10^{-3}$ mbar. This is the same order of magnitude as the threshold for spiral growth of "a" facets, which was measured by Wolf *et al.*[31] From this measurement, they estimated the mean distance between dislocations to be of order 100 μm. Thus this value can be taken as a lower bound for the crystals grown in our experiment.

When the crystal has reached a size of 10 cm^3, we let it melt slightly and the interface relaxes under the influence of gravity. As the box size (24×38 mm) is much larger than the capillary length (≈ 1 mm), the interface is horizontal at equilibrium. We then check the quality of the crystal by scanning the surface with a laser beam. If some defects intersect the free surface, they usually create cusps or grooves: the surface of a bad quality crystal looks much like an orange skin. If the scattering of the beam shows the existence of a defect, the crystal is melted to a very small size and grown again. We also check that the interface is flat (within 10^{-5} rad) on a large scale by verifying that the displacement of the reflected spot is precisely the same as that of the incident beam.

2.3. Orientation of the Crystal

The next important step in the experiment is to orient the crystal. The box which contains the crystal can be rotated around two perpendicular axes Ox and Oy using two dc micromotors inside the cell.[32] The small friction in the transmission allows operation in a pulsed mode and the box can be rotated with pulses of order 0.1 mJ. With a repetition rate of ≈ 0.5 Hz, the dissipation is small enough to operate the motors at low temperature without rewinding them with superconducting wire. The orientation of the box is monitored by two auxiliary laser beams which are reflected on two small mirrors glued on the box. The respective positions of the two auxiliary spots are located with two-elements photodiodes; the resulting accuracy in the angular measurement is 10^{-5} rad. We added a magnetic damping of vibrations by placing four little SmCo magnets close to a copper piece which is attached to the lower part of the rotating box.

At the beginning, the c axis is aligned vertically within 10^{-4} rad in the following way. The main laser beam is totally reflected at grazing incidence (4° from below) at the center of the interface. The "c" axis being off the vertical, the interface is rough and the gravity imposes a horizontal orientation. The position of the reflected spot is located with a four-elements photodiode and used as a reference for further alignments. Next, the box is rotated until the c axis of the crystal approaches the vertical: a large facet forms and at some point the beam hits the facet. In this situation, the position of the reflected spot depends on the orientation of the facet, and it is easy to run the motors until the spot reaches the reference position, so

that the facet is now horizontal. The corresponding position of the two auxiliary spots provides the required reference for further orientation. As the amplitude of the rotation is a few degrees only, it is not necessary to take into account the very small change in the interface height as the box is rotated. When the reference is determined, either one or the other motor allow to tilt the interface, and to create steps either along Ox or along Oy. The accessible angular range is $\pm 6°$ in both directions.

Finally, when the proper orientation is reached, the cell is closed with a hydraulic valve lying in the 4 K bath. This prevents any variation of the crystal size due to evaporation in the 4 K Helium bath, so that the solid-liquid interface is kept at a constant height. Our valve design is similar to the one published by Roach *et al.*[33] It is leak tight to superfluid helium at high pressure thanks to a KelF tip which is pushed by bellows against a polished stainless steel seat.

2.4. Excitation and Detection of Melting-Freezing Waves

Plane waves are excited with the ac electric field of an inter-digital capacitor evaporated on a borosilicate glass plate (periodicity 80 μm), as

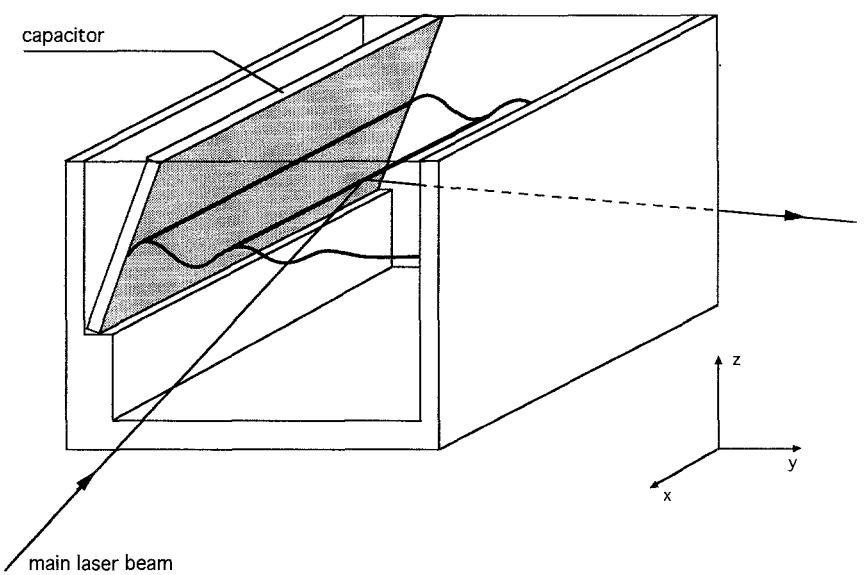

Fig. 2. Crystals are grown in a rectangular box whose width is 24 mm and whose length is 38 mm. On the tilted glass plate, an evaporated interdigital capacitor is used to generate waves travelling in the Oy direction. The incident laser beam is in the xOz plane, and is deflected in the Oy direction due to the wave. The tilt angle of the capacitor is about 25°. The box can rotate around Ox and Oy, so as to orient the lattice with respect to the free crystal surface which is forced by gravity to remain horizontal.

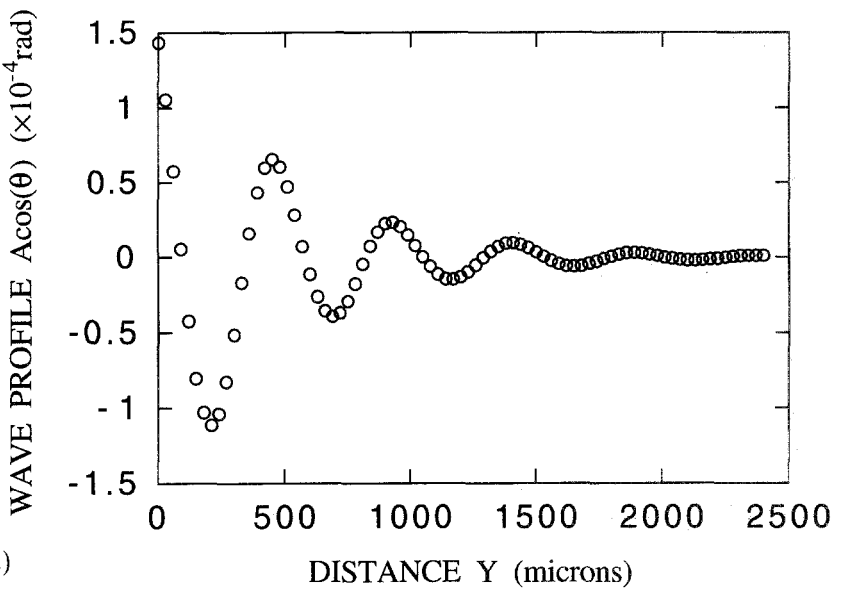

(a)

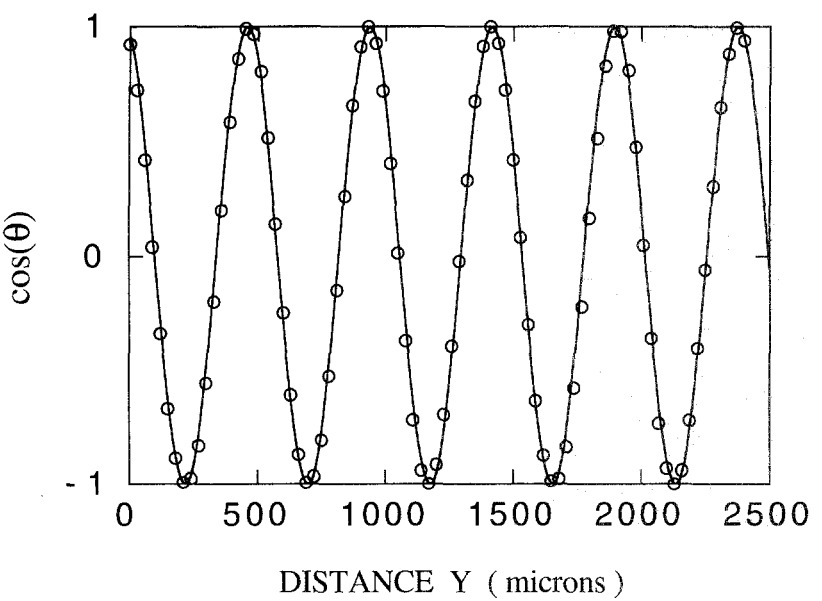

(b)

Fig. 3. A typical recording of a melting-freezing wave (here, a compression wave with $\phi = 1.2°$, $T = 0.179$ K, $f = 1119$ Hz) a) The circles are the recording of the wave profile. b) The circles are the cosine of the phase $\cos(q_R y - \theta_0)$. The solid line is a best fit with a cosine function, yielding a wavelength $\lambda = 480\ \mu$m in the present case. c) The circles are the amplitude of the wave, fitted with a decreasing exponential. The corresponding peak-peak height amplitude varies from 400 Å to 4 Å.

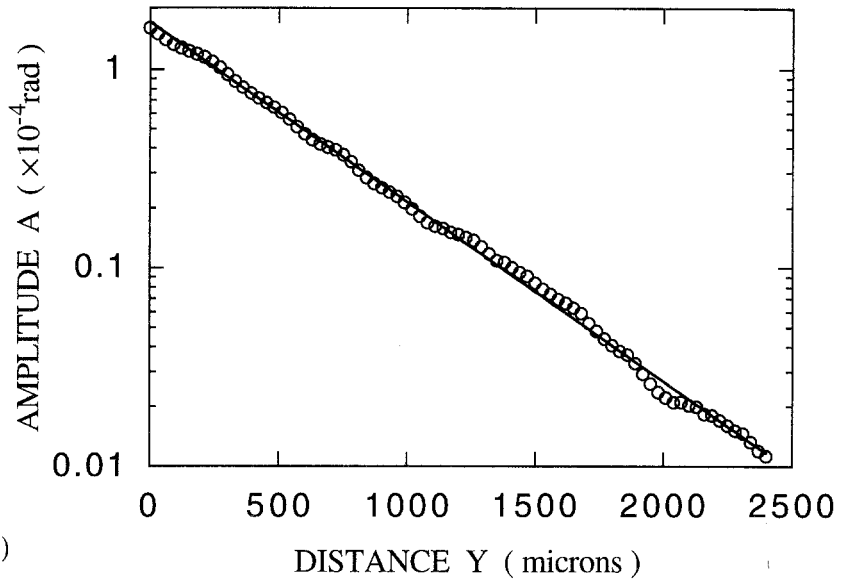

(c)

Fig. 3. *(Continued)*

done previously by Wang and Agnolet.[34] The dissipation in the capacitor is of the order of 30 μW for a typical ac voltage (1 KHz, 100 Vpeak-peak). Together with the 300 K radiation, this prevents us from observing waves below 40 mK. As the contact angle of the solid-liquid interface with the walls is about 135°, a meniscus forms near the plate. In order to obtain a flat surface with a well defined orientation, a continuous voltage (≈ 150 V) is also applied.

The plate is parallel to Ox and the wave vector $\vec{q}$ is along Oy (Fig. 2). The profile of the wave is recorded by scanning the surface along Oy with the main laser beam. The angle of incidence is 4°, and the beam is totally reflected. The reflection direction is modulated by the wave, and measured with a position detector. This is a two-elements photodiode connected to a lock-in amplifier. Our method is very sensitive to the modulation of the surface orientation. We used a maximum amplitude of about 2×10^{-4} rad or 10^{-2} degree, i.e., much smaller than the tilt angle. This corresponds to a maximum height modulation of order 200 Å. Our limiting sensitivity is of order 10^{-6} radians or 1 Å in height. The double phase lock-in amplifier provides both the cosine of the phase $\theta(y)$ and the amplitude $A(y)$ of the wave (Fig. 3). We can thus fit independently $\cos\theta$ with a cosine function $\cos(q_R y + \theta_0)$ and A with a decreasing exponential $A_0 \exp(-q_I y)$. We finally obtain both the real part q_R and the imaginary part q_I of the wavevector q.

The complete dispersion relation for melting-freezing wave is:[35]

$$\omega^2 = \frac{\rho_L}{(\rho_c - \rho_L)^2}\left[\gamma q^3 + (\rho_c - \rho_L)\, gq - i\frac{\rho_c}{k}\omega q\right] \tag{4}$$

where γ is the surface stiffness, g the gravity. As previously,[1] we use the symbol k for the isothermal mobility. It is defined as the ratio of the difference in chemical potential (per unit mass) across the interface to the growth velocity if there is no temperature difference ($k = v/\Delta\mu$ if $\Delta T = 0$). The same notation has been used by Nozières,[4] while the heavier notation (Km) was used by various authors.[21,34,45]

In the limit of small wavelength and small damping, one recovers the usual dispersion relation for capillary waves: ω is proportional to $q^{3/2}$. In the same limit the mobility is given by:

$$k = \frac{1}{3}\frac{\rho_c \rho_L^{1/3}}{(\rho_c - \rho_L)^{2/3}}\frac{\omega^{1/3}}{\gamma^{2/3} q_I} \tag{5}$$

The mobility can thus be obtained from the damping, provided that one checks that q_I varies like $\omega^{1/3}$. Such power law dependencies have been measured previously for rough surfaces by Keshishev *et al.*[20] In order to

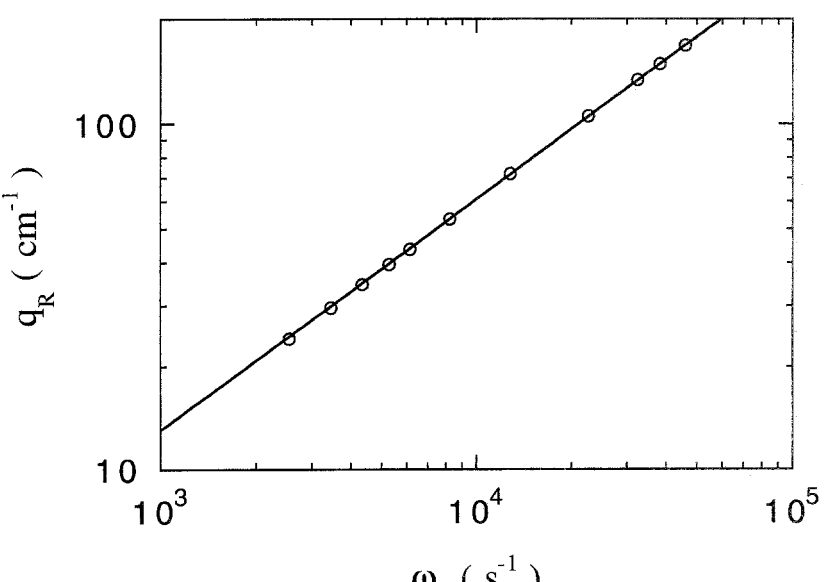

Fig. 4. Dispersion relation $\omega(q_R)$ for melting-freezing waves at fixed temperature (0.15 K) and orientation (1°). The circles are experimental data and the solid line corresponds to a $q^{3/2}$ dependence, which is expected for a capillary wave. This shows that the gravitational term in the dispersion relation is very small.

check our method, we made systematic measurements of q_R and q_I at fixed tilt angle (1°) and temperature (150 mK), for frequencies ranging from 0.4 to 9 KHz. As shown on Figs. 4 and 5, we find a good agreement with the expected theoretical dependencies $q_R(\omega)$ and $q_I(\omega)$.

In order to analyze our measurements, we kept the full expression for the dispersion relation (Eq. 4). Nevertheless, in order to increase the accuracy, the frequency was chosen in most further experiments such that the gravitational term in Eq. 4 is a small correction, and such that the damping is weak ($q_R \ll q_I$).

As we shall see in Sec. 4, the damping strongly increases as a function of temperature. At high temperature where k is less than 1 s/cm, it is not possible to propagate waves, nor consequently to measure γ or k by our method. At low temperature, the damping is weak and the measurement of γ is easier, although the amplitude of parasitic vibrations is larger. If the damping is very low, the wave is reflected at the wall opposite to the capacitor, and we obtain oscillations of the amplitude which show the existence of standing waves (Fig. 6). If the attenuation length is not too large compared to the size of the crystal, k can still be obtained by fitting the signal with the sum of two weakly damped waves propagating in

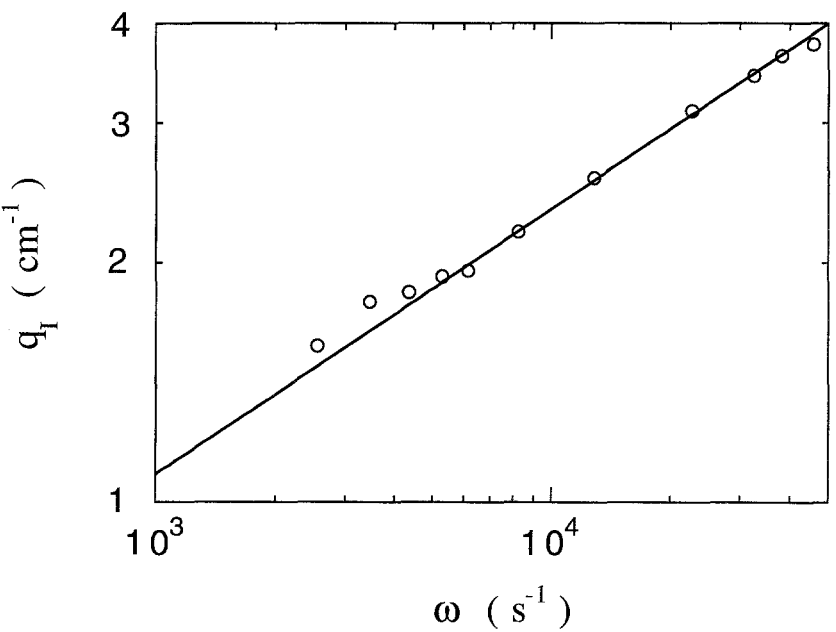

Fig. 5. The imaginary part q_I of the wave vector as a function of ω, for melting-freezing waves at fixed temperature (0.15 K) and orientation (1°). The circles are experimental data and the solid line corresponds to the theoretical dependence $\omega^{1/3}$.

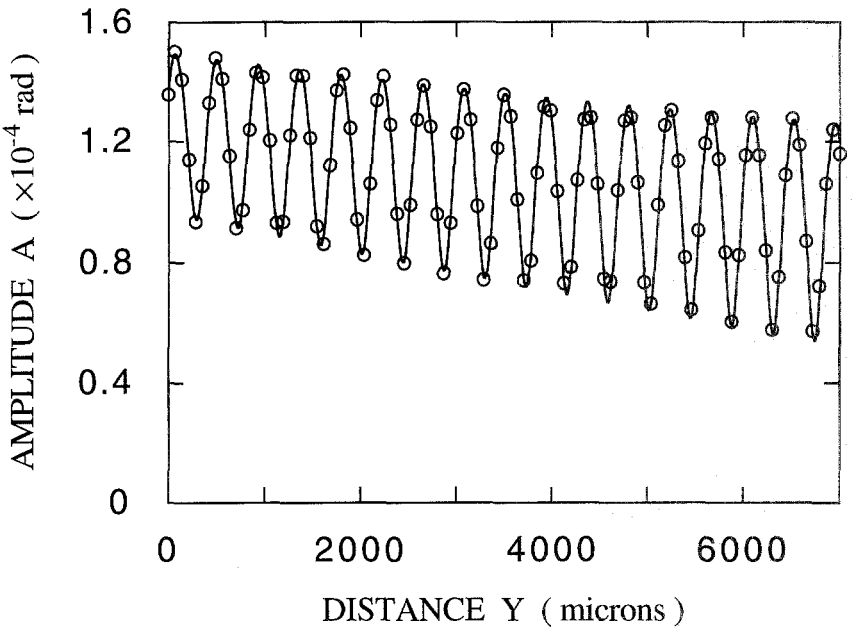

Fig. 6. The circles are the recording of the amplitude of a melting-freezing wave, for a low damping (rough orientation, $T = 0.28$ K, $f = 908.3$ Hz). The oscillations of the amplitude show the existence of a standing wave. The solid line is a best fit with a function $f(y)$ which is the resulting amplitude for two weakly damped waves travelling in opposite directions.

opposite directions (Fig. 6). If the mobility k is larger than 100 s/cm, there is too much interference with reflected waves and the method is not accurate. As a result, k can only be measured in the range 1–100 s/cm. For a tilt angle $\phi = 8°$, this corresponds to a temperature range 0.2–0.5 K. Moreover, the mobility is also strongly orientation dependent, so that the accessible temperature range for small tilt angle (e.g., $\phi = 0.5°$) is rather 0.1–0.2 K.

3. THE STIFFNESS OF VICINAL SURFACES

3.1. The Crossover from Stepped to Rough Behavior

We have recorded the propagation of several hundred waves on the surface of many crystals for various temperatures, orientations and frequencies. Some of our results are presented on Fig. 7 which shows that the surface properties drastically change as a function of angle. Indeed, above 4°, the surface is nearly isotropic ($\gamma_{\parallel} \approx \gamma_{\perp} \approx 0.2\,\text{erg} \cdot \text{cm}^{-2}$). In contrast, below about 1°, the anisotropy is very large: the transverse stiffness $\gamma_{\perp}$ diverges while $\gamma_{\parallel}$ vanishes. We have already published a preliminary report on this effect[23] which is observed for the first time. The crossover from anisotropic

to isotropic takes place at $\phi_c \approx 2.5°$, in very good agreement with our prediction.[1] We thus interpret our results as experimental evidence for a crossover from stepped to rough behavior, which occurs where the step width w is comparable to the mean distance $d = a/\tan\phi$ between steps.

In Ref. 1 as in earlier publications,[31,36] we used the continuous sine-Gordon theory[4,5] with the explicit hypothesis that, in the case of helium, the coupling of the surface to the lattice is weak. Physically this means that the anchoring potential acts weakly on the surface. At a step, the interface height changes smoothly from 0 to a over a distance which is much larger than the lattice spacing a. The height can thus be described with a continuous variable $z(x)$, and the energy associated with a step is small (more specifically, $\beta \ll \alpha a$). Most solid-liquid interfaces are expected to be weakly

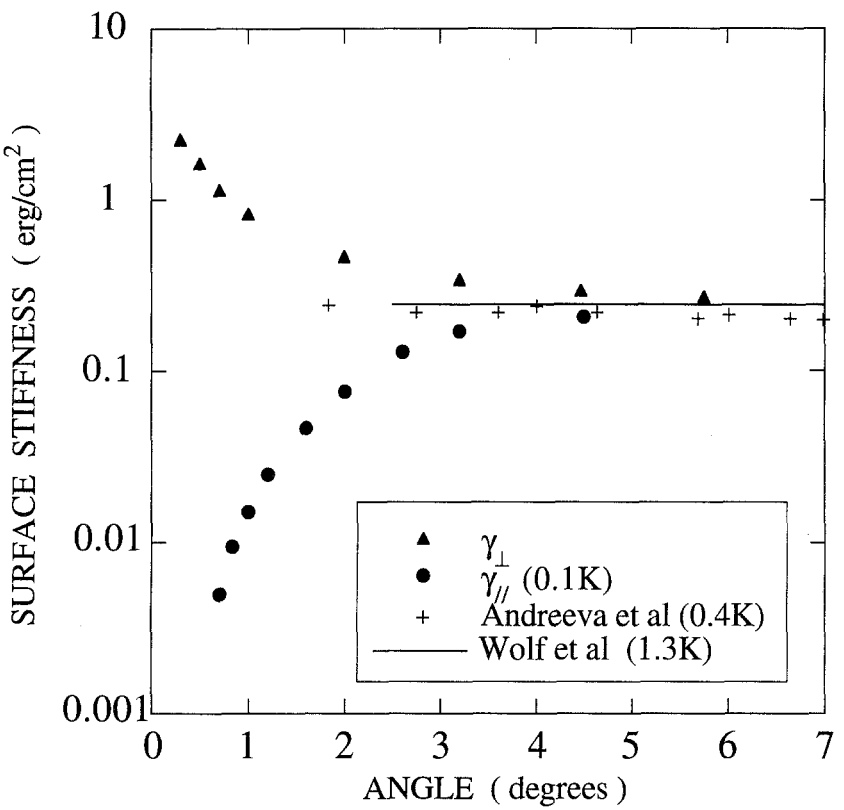

Fig. 7. The two components of the surface stiffness as a function of the tilt angle ϕ. As ϕ tends to zero, $\gamma_\perp$ diverges while $\gamma_{||}$ vanishes. Above 4°, our low temperature measurements agree with other data obtained at higher temperature by Andreeva *et al.*[21] and Wolf, Gallet *et al.*[31,36]: a crossover from stepped to rough behaviour has occurred.

coupled. Furthermore, numerical simulations[37] show that, in helium, the liquid-solid interface is much larger than the atomic spacing so that the width of a step cannot be small. Simulations also allow to understand the exact role of the large zero point motion of helium atoms in this weak coupling. The opposite situation would be a metal to vacuum interface which is expected to be strongly coupled with high energy sharp steps ($\beta \approx \alpha a$).

The weak coupling hypothesis allowed Nozières[4,5] to describe the step profile by the simple analytic formula

$$z(x) = \frac{2a}{\pi} \tan^{-1}\left[\exp\left(\frac{x}{\xi}\right)\right] \tag{6}$$

where ξ is the correlation length on c surfaces. Furthermore, we explained in Ref. 1 that, if w is defined as the distance on which the surface height goes from $0.1a$ to $0.9a$, w is about 4ξ and terraces are not well defined if their size d is less than about $3w$. Although Nozières' theory is strictly valid close to the roughening temperature $T_R = 1.30$ K only, an extrapolation was used in Ref. 1 so as to predict the low temperature value w_0 of the step width and the crossover angle $\phi_{c0} \approx a/3w_0$. We had found $\xi_0 \approx 2a$, $w_0 \approx 8a = 24$ Å and a crossover around 2.5°. This is precisely what we also found experimentally. We believe that such a crossover from stepped to rough is a very general phenomenon which should be observable on any weakly coupled crystal surfaces, in particular on most liquid-solid interfaces. The only unpredicted result is the large width of the crossover: it extends from 1 to 4° and is thus wider than in Ref. 1 where it was arbitrarily drawn sharp. We shall consider this crossover width at the end of Sec. 3.

The next question is the temperature dependence of this crossover. In Ref. 1 we had predicted that as T increases, the crossover angle $\phi_c(T)$ should decrease to zero at T_R where the step width is infinite. The initial slope of $\gamma_{||}$ should also increase since it is proportional to the step interaction (see 3.2). We have observed such a general trend (Fig. 8). However, as explained in Sec. 2, we could not study the crystallization waves both at low angle and high temperature. The full temperature evolution between 0.4 and 1.3 K thus remains to be observed. When the damping of crystallization waves is too high, one should probably look again at equilibrium crystal shapes, a difficult experiment which is presently tried by A. V. Babkin[15] in Helsinki.

Let us now describe the theory in some more details, in order to understand what is the meaning of the good agreement between experimental results and theoretical prediction. In the sine-Gordon model, the lattice potential is renormalized from its microscopic value at the starting length

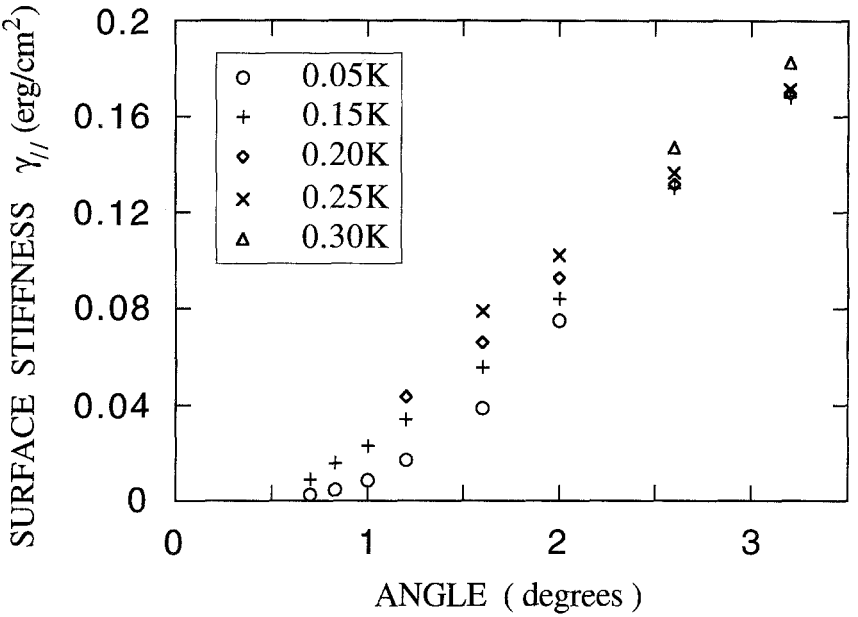

Fig. 8. The angular variation of the longitudinal component of the surface stiffness $\gamma_{||}$ at successive temperatures. As T increases, the initial slope increases and the crossover angle to rough behaviour decreases.

scale $\Lambda_0^{-1} \approx 2.5\xi_0$ to its macroscopic value at large length scale. If T is smaller than the roughening temperature T_R, this macroscopic value diverges so that the lattice potential locks the interface on the lattice. However, at a scale smaller than Λ_0^{-1}, there is no renormalization at all, and consequently no difference between a facet and a rough interface. This is precisely what happens if the tilt angle is larger than a critical value ϕ_{c0}: whatever the temperature, the terraces are too small for any renormalization to start, i.e., any influence of the neighboring facets to show up in the properties of the vicinal surfaces. We indeed found that above about 4° the present experimental results agree with those by Wolf, Gallet *et al.*[31,36] and by Andreeva *et al.*[21] despite the fact that the temperature ranges were different in all these experiments. At large angle, the variation of γ was found to be $0.245\ (1 - 12\phi^2)$ by Wolf, Gallet *et al.*[31,36] and it is now well established as non-singular, i.e., independent of the existence or evolution of facets in the c direction. The critical variation of γ shows up only for tilt angle smaller than ϕ_{c0}. In this domain, we showed in Ref. 1 that our model is consistent with the old measurements performed close to T_R by Babkin *et al.*[38]

Now, at $T = 0$ there are no thermal fluctuations, consequently no renormalization either. In Ref. 1, we thus identified the unrenormalized

surface with the $T=0$ surface. That is the way we obtained $w_0 = 8a$, by using the value of ξ_0 fitted on measurements close to T_R. As a consequence, the crossover from stepped to rough behavior at low temperature was predicted to occur at the same angle ϕ_{c0} as the beginning of the critical angular domain for the surface stiffness close to the roughening temperature $T_R = 1.3$ K (see Figs. 5 in Ref. 1). This is precisely what is now verified experimentally. We have thus shown that the unrenormalized surface is indeed similar to the surface at zero temperature. This in turn suggests that the sine-Gordon theory is valid at any scale, as expected if the coupling is small enough, even at a microscopic scale.

3.2. The Step Free Energy β and the Adsorption of ^{3}He Impurities

Having understood the existence of a crossover from stepped to rough, we have tried to check Eqs. 2 and 3, that is to measure the step energy and the step interactions. Let us start with the step energy. Fig. 9 shows a plot of the inverse stiffness $1/\gamma_\perp$ as a function of tilt angle. There are two sets of data, one corresponding to ultrapure helium 4 with a concentration in

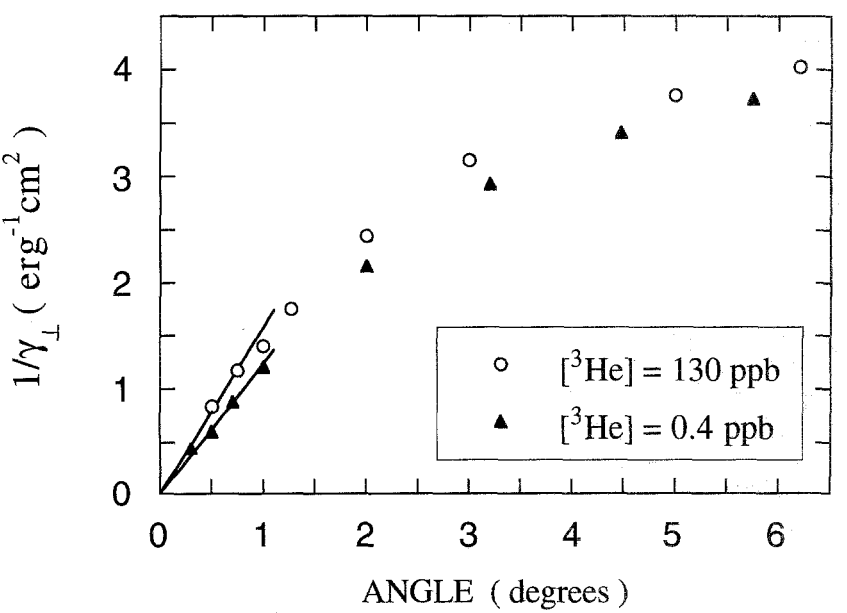

Fig. 9. $1/\gamma_\perp$, the inverse of the transverse component of the surface stiffness, as a function of the tilt angle ϕ, for two ^{4}He samples with different purities. Both sets of data vanish linearly at small tilt angle ($\phi < 1°$), as expected theoretically. From the slope at the origin, we infer the value of the step free energy β (see text).

helium 3 impurities of 4×10^{-10} only, and the other one with normal purity ($[^3\mathrm{He}] = 1.3 \times 10^{-7}$). In both cases, the temperature range of the experiment was typically 50–250 mK for small tilt angle ($\phi < 1°$) and 200–400 mK for large tilt angle ($\phi > 2°$).

As can be seen on this figure, we have found that, below about 1°, $1/\gamma_\perp$ is linear as a function of ϕ, as predicted by Eq. 3. We conclude that the step free energy is

$$\beta/a = (14 \pm 0.5) \times 10^{-3}\ \mathrm{erg \cdot cm^{-2}} \tag{7}$$

This value corresponds to the ultrapure sample and it decreases by 20% when 0.13 ppm impurities are present.

Let us first discuss the ultrapure case. In the temperature range from 40 to 250 mK, the step energy was found constant within the error bar of the measurements. Eq. 7 thus gives the low temperature value of the step energy. The agreement with our predictions[1] is surprisingly good. Indeed, $\beta/a = 0.057\alpha$ is not only very small compared to α, it is very close to the prediction $\beta/a = 17 \times 10^{-3}\ \mathrm{erg \cdot cm^{-2}}$ which was obtained in Ref. 1. We had there extrapolated the theory very far from its domain of validity, i.e., very far from the region near T_R where Gallet *et al.* measured step energies of order $10^{-4}\ \mathrm{erg \cdot cm^{-2}}$ only. We here obtain a quantitative proof that Nozières' theory is not only valid close to the roughening transition but also away from it, because the weak coupling hypothesis is correct at all scales and all temperatures.

Let us now come to the influence of impurities. As explained in more detail in Ref. 27, we believe that some adsorption of helium 3 atoms takes place at the liquid-solid interface, and preferentially on the steps. As can be seen on Fig. 9, we also observed a change in the surface stiffness γ at large angle. At such large angles the stiffness is nearly isotropic and can be identified with the surface tension α. We found that the change $\Delta\alpha = \alpha(0.4\ \mathrm{ppb}) - \alpha(130\ \mathrm{ppb})$ decreases from about $15 \times 10^{-3}\ \mathrm{erg \cdot cm^{-2}}$ around 0.2 K to zero above 0.4 K. We understand the low temperature change $\Delta\alpha$ as due to the adsorption of helium 3 atoms, an effect which had been predicted by J. Treiner.[39] The fact that impurities desorb around 0.4 K is easily interpreted by adjusting the binding energy. We find it to be 4.3 K, a slightly larger value than predicted by Treiner.[39] We also found that the 20% change in step energy $\Delta\beta$ is constant in the temperature interval 0.1–0.2 K. Quantitative agreement was found if the adsorption saturates below 0.2 K when a maximum surface density of 0.4 monolayer is reached. Our observation of a constant step energy also means that steps do not create new surface states, they only increase the local binding energy by a small amount, about 10 mK. Although this whole picture looks in

reasonable agreement with Treiner's calculations, a much more systematic study is needed for a more precise understanding of helium 3 adsorption. Among hypotheses which we could not check is one stating the existence of a large number of vortices in the pores of our sintered silver heat exchangers. We assumed that these vortices trap most of the helium 3 impurities below 0.3 K, as observed by Varoquaux *et al.* in a different context.[40] We finally concluded that our ultrapure sample is pure enough for the crystal surface to be totally free of impurity adsorption.

3.3. The Interaction Between Steps

Let us now consider the limiting behavior of $\gamma_{||}$ at small tilt angle. As shown on Fig. 10, $\gamma_{||}$ reaches very small values as ϕ tends to zero. Unfortunately, our measurements are restricted to $\phi > 0.7°$. This prevents us from demonstrating directly the linear dependence of $\gamma_{||}(\phi)$ which is expected for $1/d^2$ interactions. We still think that our results provide a good evidence for the existence of mixed elastic and entropic interactions. Indeed, we have calculated these interactions and found very good agreement with our measurements, especially at the smallest angle we have reached ($\phi = 0.7°$) in the whole temperature range 0.05 to 0.15 K.

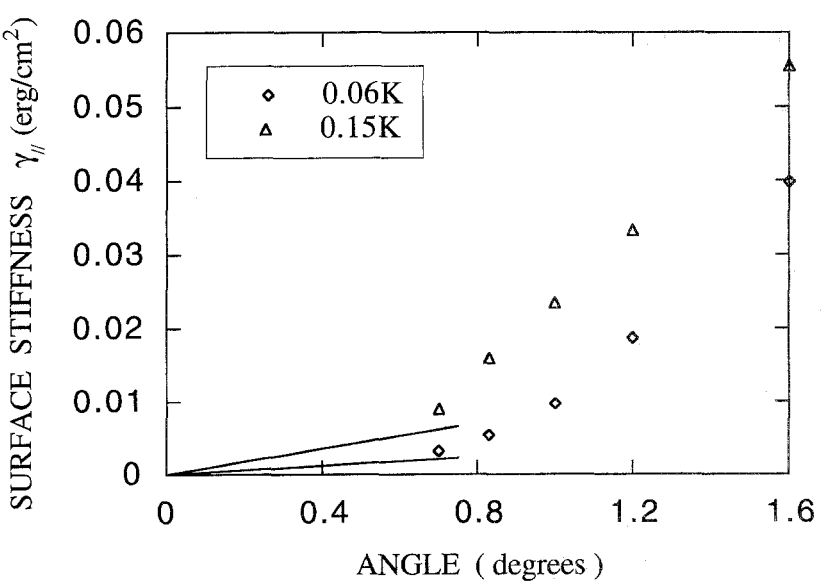

Fig. 10. $\gamma_{||}$ as function of the tilt angle ϕ and for small values of ϕ. In the limit of vanishing tilt angle, our measurements are consistent with the linear variation (solid line) which can be calculated from the magnitude of step interactions.

We wish first to explain why our measurements could not be performed at lower angle. Of course, not all recordings were as clean and regular as shown on Fig. 3. We only kept for analysis those recordings where no significant drift in the base line was observed and where the wavelength was constant over several periods. It appeared that the latter criterion was met more easily in the transverse geometry than in the longitudinal one. We think that this is a consequence of the residual vibrations. Indeed, if the steps are oriented strictly perpendicular to the wave vector $\vec{q}$, we exactly measure $\gamma_{||}$. Similarly, $\gamma_{\perp}$ is measured if the steps are strictly parallel to $\vec{q}$. In the general case where the steps are tilted by an angle θ with respect to $\vec{q}$, we measure a stiffness

$$\gamma(\theta) = \gamma_{||} \sin^2 \theta + \gamma_{\perp} \cos^2 \theta \tag{8}$$

In the transverse geometry, a small misorientation has no drastic consequence because θ is close to 0 and $\gamma_{\perp} \gg \gamma_{||}$. On the contrary, in the longitudinal geometry, mechanical vibrations are enough to introduce an important correction in the measurement of $\gamma_{||}$ as soon as the anisotropy is large, i.e., at small ϕ. We observed variations of the period along the scan because the vibration level is not homogeneous on the whole surface of the cell (there are nodes according to the shape of resonant modes). After optimizing the mechanical stability of our experiment (bellows on pumping lines, air springs, magnetic friction on the rotating box), we could measure $\gamma_{||}$ down to 0.7° where it is less than 1% of $\gamma_{\perp}$ but not lower in angle.

Let us now come to the interactions and first rule out the possible existence of $1/d$ interactions. Suppose that the interaction amplitude is ε/d. Instead of vanishing linearly as predicted by Eq. 2, the surface stiffness $\gamma_{||}$ would tend to the constant $2\varepsilon/a^2$.[1,18] Close to the facet edge, the equilibrium crystal shape would then have a constant radius of curvature R instead of a vanishing one (R is proportional to γ). When looking at such equilibrium shapes with ordinary optical methods it is indeed hard to distinguish between these two possible shapes. Our experiment shows for the first time that the surface stiffness $\gamma_{||}$ vanishes at small angle, so that if $1/d$ interactions exist, they are very small: we have measured values of $\gamma_{||}$ as low as 2×10^{-3} erg $\cdot$ cm^{-2} so that an upper limit for ε/a^2 is 10^{-3} erg $\cdot$ cm$^{-2} \approx 4 \times 10^{-3}\,\alpha$. On the contrary, our results are consistent with $1/d^2$ interactions with a reasonable amplitude.

Indeed there are two possible origins for such interactions.[1,4] The first one is elastic and results from the overlap of strain fields around neighboring steps. Between two steps a distance d apart, the interaction energy per unit length was calculated by Marchenko and Parshin[24] and reformulated by Nozières[4] as

$$\frac{\delta_{el}}{d^2} = \frac{2}{\pi} \frac{(1-\sigma_P^2)(\vec{f}_1 \cdot \vec{f}_2)}{Ed^2} \tag{9}$$

In this formula, $\vec{f}_1 = (f_1^x, f_1^z)$ and $\vec{f}_2 = (f_2^x, f_2^z)$ are the two force doublets which create each strain field around each step.[4] The z component is perpendicular to the terraces and equal to the surface stress π_s. The x component is parallel to the terrace and difficult to calculate but it should have a similar amplitude. The surface stress is a difficult quantity to measure. A reasonable order of magnitude is the surface tension $\alpha = 0.245$ erg $\cdot$ cm^{-2}, although Edwards *et al.*[41] obtained the indirect estimate $\pi_s \approx 0.6$ erg $\cdot$ cm^{-2}. We thus estimate the product $\vec{f}_1 \cdot \vec{f}_2$ to be $2\alpha a^2$. From the value of Young's modulus[42] $E = 3.05 \times 10^8$ erg/cm^3 and that of Poisson's ratio $\sigma_P = 1/3$, we estimate the elastic interaction between two steps to be

$$\delta_{el} = 2.0 \times 10^{-25} \text{ erg} \cdot \text{cm} \tag{10}$$

In the case of a stepped surface, one has to integrate over the infinite number of steps and one finds a total elastic interaction $(\pi^2/6)\,\delta_{el}$ between each step and all its neighbours.

Now, the crossing of steps is forbidden because it would create overhangs.[1,4] As a consequence, the step fluctuations are limited by the presence of other steps. This is the physical origin of the other interaction, often called "entropic" or "statistic ". Its exact amplitude is now known to be

$$\frac{\delta_s}{d^2} = \frac{\pi^2}{6} \frac{(k_B T)^2}{\beta} \frac{1}{d^2} \tag{11}$$

Equation 11 is taken from the work of Akutsu *et al.*,[26] where we replaced the step stiffness by the step free energy β because, as justified below, we assume that the kink density is high so that the stiffness and the free energy are the same isotropic quantity. Equation 11 could also be derived from the work of Bartelt, Williams *et al.*[9] provided that an unfortunate numerical error is corrected. Indeed Bartelt *et al.* used the previous work by Jayaprakash *et al.*[25] where the hopping matrix element should be doubled.[26] We assume that the kink density is high because we estimate the kink energy ε_k as a few mK only. Indeed, as explained above, the weak coupling leads to a step energy which is small compared to the surface energy ($\beta \ll \alpha a$). For the same reason, the kink energy should be small compared to the step energy ($\varepsilon_k \ll \beta a \ll \alpha a^2$). Indeed the meaning of weak coupling is that the lattice potential is small: little energy is required for the surface to lie in between its periodic positions of minimum potential energy. This is why steps minimize their energy by relaxing their width to

a large value: it costs a small potential energy and it gains a lot of surface area. Similarly, we expect kinks to be wide defects with an energy smaller than the step energy. Considering that $\beta a = 0.057\ \alpha a^2 = 91$ mK, we thus estimate the kink energy to be $\varepsilon_k \approx 0.057\ \beta a = 5.2$ mK. Since the minimum temperature is 40 mK in this experiment, we can consider steps as continuous isotropic defects with a high density of kinks.

This assumption being justified, we can calculate the entropic interaction since we have measured the step energy β. We find

$$\delta_s = 7.47 \times 10^{-23}\ T^2\ \text{erg} \cdot \text{cm} \tag{12}$$

Furthermore, we find $\delta_s = (\pi^2/6)\ \delta_{\text{el}}$ at $T = 66$ mK. As a consequence, we are in an intermediate regime where the two interactions have comparable amplitudes and we need an interpolation formula since they do not add linearly. Following Jayaprakash *et al.*,[25] Bartelt, Williams *et al.*[9] proposed the following formula for the total interaction:

$$\delta = \frac{\delta_s}{4}\left[1 + \sqrt{1 + \frac{2\pi^2}{3}\frac{\delta_{\text{el}}}{\delta_s}}\right]^2 \tag{13}$$

In our preliminary report,[23] we had tried to fit the observed temperature variation of the longitudinal stiffness $\gamma_{||}$ with Eq. 13 and with two adjustable parameters: the forces f_i and the numerical coefficient in front of the entropic interaction. We had found agreement with Eqs. 9, 11 and 13. However, in view of the large error bars found at the end of such a fit, we here prefer to show that our results are well described by the above numerical estimates for δ_{el} and δ_s together with Eq. 13.

As shown on Fig. 10, we observed the initial slope of $\gamma_{||}$ to increase with temperature. The straight lines are drawn according to Eqs. 2, 10, 12 and 13 and agree with the experimental results. Fig. 11 shows better evidence that our description of the interactions is correct, especially its temperature dependence. From this figure, it is also clear that our smallest angle is not yet small enough: at 0.7° the asymptotic linear regime for $\gamma_{||}$ versus ϕ is only marginally reached. If experiments could be performed at 0.5° or below, the value of $\gamma_{||}/\phi$ would be independent of ϕ, all plots would superimpose on each other whatever the angle, and an even better agreement would probably be found. The lack of such very small angle data is an additional reason why here we prefer to show that our results are very close to a reasonable estimate of mixed elastic and entropic interactions, than to try again to extract an exact value for these interactions from our data.

One could argue that the above analysis neglects other possible sources of interactions. The main one is the hydrodynamic interaction

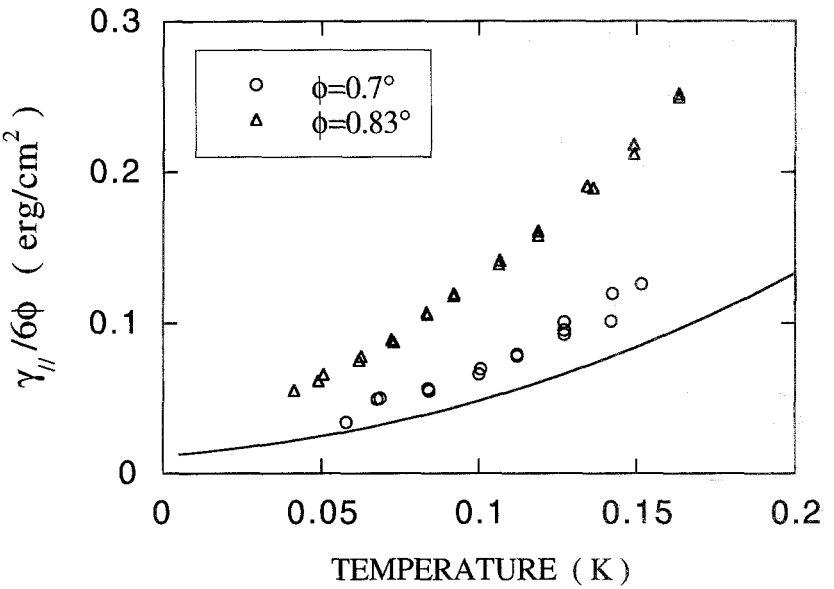

Fig. 11. $\gamma_{||}/6\phi$ for two different orientations as a function of the temperature. The solid line is the theoretical prediction for the interaction δ/a^3 using equations 10, 12 and 13.

which was predicted by M. Uwaha.[11] Physically, it originates in the overlap between the flow fields associated with the fluctuations of each step, more precisely the cross term in the kinetic energy associated with these fields. Uwaha calculated this hydrodynamic interaction in the quantum limit of zero point fluctuations and in the classical limit of thermally excited fluctuations. He predicted that this new interaction is repulsive again, and intermediate between $1/d$ and $1/d^2$. We estimated it numerically and found that it should contribute by 5% only to our smallest experimental value of $\gamma_{||}$. This is why we neglected it.

Let us finally comment on the width of the crossover. At the time of Ref. 1 we had no idea of what it could be. Since then, Nozières calculated the shape of this crossover for a tilted sine-Gordon model at $T=0$ with no elastic interactions. He indeed found that the crossover width is large.[43] But of course, it would be very useful for us to have a full theory at finite T and variable angle including elastic interactions. We could then deduce precise values of both interactions from a fit of our data, even though they do not extend to very low angle. The underlying physics is interesting. For instance, the description of entropic interactions by Eq. 11 is valid when the step width is small compared to the mutual distance between steps. A simple way to describe the interaction for steps with a finite width w could be to assume that the step fluctuation amplitude is limited to $(d-w)$

instead of d, consequently to replace d^2 by $(d-w)^2$ in Eq. 11. This would lead to a quadratic correction to the linear variation described by Eq. 2. However, such a simple treatment would neglect possible deformations of the step profile when it approaches a neighbour. A correct treatment needs a much more elaborate theory and we hope that our experiments trigger further efforts along such lines.

4. MOBILITY

We now turn to the results which concern the mobility k of the solid-liquid interface. Since our temperature is low, we neglect the possible effect of heat currents and we identify the mobility with the isothermal growth coefficient $k = v/\Delta\mu$, where v is the interface velocity and $\Delta\mu = (\mu_L - \mu_C)$ is the difference in chemical potential per unit mass across the interface. We first discuss the case of completely rough surfaces at large tilt angle, which we used as a test for our experimental technique. We then present our results for vicinal surfaces. We show that they can be interpreted in the framework of a theory developed by Nozières and Uwaha,[28] which is based on the scattering of thermal phonons by the steps.

4.1. The Mobility of Rough Interfaces

The mobility of a rough interface has been extensively studied, both experimentally and theoretically. Experiments[20,34,44] have shown that the temperature dependence of the inverse mobility or growth resistance k^{-1} can be described as follows:

$$k^{-1} = A + BT^4 + C\exp(-\Delta/T) \tag{14}$$

The second and the third terms respectively account for phonons and rotons (Δ is the roton gap). As our experiments are performed below 0.5 K, we are mainly interested in the phonon contribution. Experimental values[20,44] of B range from 2.7 to 3.5 cm s^{-1} K^{-4}, in good agreement with theoretical calculations by Bowley and Edwards (3.06 to 3.32 cm s^{-1} K^{-4}).[45] The origin of the first term in (14) is not well understood. As this excess growth resistance changes from one crystal to another, also from one run to another with the same crystal, Keshishev *et al.*[20] suggested that it is due to defects within the crystal.

Since the mobility of rough surfaces is reasonably well understood, we first measured k for a crystal with a large tilt angle ($\phi = 15°$), and we checked that our experimental set-up provides us with accurate and reliable data. The experimental measurements are shown on Fig. 12, where the

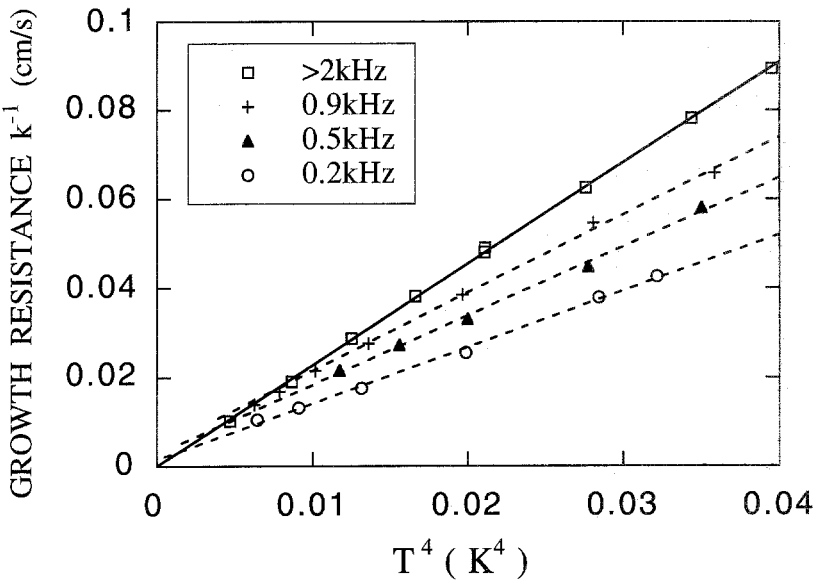

Fig. 12. The growth resistance of a rough surface ($\phi = 15°$) as a function of T^4, for different frequencies. At high frequency ($f > 2$ kHz), one finds the usual T^4 dependence (solid line). At low frequency and high temperature a departure from this law is observed: the growth resistance is reduced. From the crossing of the broken lines with the solid line, we determine crossover temperatures where the scattering of phonons is shown to change from ballistic to hydrodynamic (see text).

growth resistance is plotted as a function of T^4. In order to emphasize the phonon contribution, the small roton contribution $C\exp(-\Delta/T)$ has been subtracted (C has been taken equal to the value given by Wang and Agnolet).[34] In the whole temperature range of Fig. 12, the roton contribution is at most 5%.

At high frequency ($f > 2$kHz), the temperature dependence of k^{-1} is clearly like T^4, with no constant term (we find $A < 10^{-3}$ cm s^{-1}). The coefficient B is found to be equal to 2.27 cm s^{-1} K^{-4}, i.e., a little smaller than some other measurements.[20,44] Since Andreeva *et al.*[21] showed that B depends on orientation, even for rough surfaces, we believe that the agreement with previous experiments is quite satisfactory.

More interesting is the frequency dependence of the dissipation. Fig. 12 shows that above 0.3 K, the growth resistance decreases when f decreases. We think that the explanation is the following:[45] at high frequency, the wavelength λ_c of the capillary wave is smaller than the mean free path l_{mfp} of thermal phonons in the crystal (a fortiori in the liquid). All phonons are thus ballistic, and contribute to the dissipation. When f decreases, λ_c

increases, so that more and more crystal phonons are at rest in the frame of the interface. These hydrodynamic phonons no longer contribute to the growth resistance k^{-1}. If all phonons are hydrodynamic, and if the dissipation is due to the viscosity η of the phonon gas, the imaginary part q_I of the wave vector is $q_I = (4\eta/3\gamma)\omega$.[45] So q_I varies like ω instead of $\omega^{1/3}$ in the ballistic case. At $T = 0.41$ K and for frequencies in the range 200–1000 Hz, we find that the crystal phonons contribution to q_I varies roughly like $\omega^{0.7}$. This is consistent with a situation where some crystal phonons are ballistic and some hydrodynamic.

From our data, it is also possible to estimate $l_{\text{mfp}}(T)$. Consider the curves $k^{-1}(T)$ at a fixed frequency, i.e., at fixed wavelength λ_c. At low enough temperature, phonons are ballistic and $k^{-1} = BT^4$. The change in the curve $k^{-1}(T)$ occurs at a temperature T_{hyd} where some phonons become hydrodynamic. Thus it seems reasonable to suppose that $l_{\text{mfp}}(T_{\text{hyd}}) = \lambda_c$. In order to estimate T_{hyd}, we suppose that, in the high temperature range 0.3–0.45 K, $k^{-1}(T)$ varies linearly with T^4 with a different slope. This is somewhat arbitary, but simple and good enough for our purpose. T_{hyd} is then taken from the intercept of these two linear regimes. We thus obtain: $l_{\text{mfp}}(0.2\text{ K}) \approx 2.4$ mm and $l_{\text{mfp}}(0.3\text{ K}) \approx 0.9$ mm. These values agree with previous estimates.[46]

It should also be noted that such a change in the temperature variation of the growth resistance has been observed at a lower frequency by Wang and Agnolet.[34] Our data strongly support their interpretation that a crossover occurs from ballistic to hydrodynamic phonons as a function of temperature. It is now clear that this crossover is also frequency dependent, as predicted by Bowley and Edwards.[45]

4.2. Mobility of a Vicinal Interface

For a facet, growth can only occur through nonlinear mechanisms such as spiral growth or 2D nucleation of terraces. If the orientation approaches the c axis, the mobility is expected to become very small and to vanish at $\phi = 0$. When ϕ is very small, one expects the growth to occur layer by layer, and the mobility to be proportional to the density of steps $n \approx \phi/a$. k can thus be expressed as:

$$k = na\,k_s \tag{15}$$

where k_s is now the mobility of a single step. In Eq. 15, the lattice spacing a is introduced to make k_s homogeneous to k, so that the velocity of a step v_s is equal to $k_s\,\Delta\mu$. Of course, such a description should be valid only if steps do not overlap ($n < 1/3w$). As stressed by Nozières and

Uwaha[28] (NU), this condition is necessary but not sufficient. The steps respond independently to the applied force if they scatter the thermal phonons independently. These phonons behave as wave packets with a size of order $q_{\rm ph}^{-1} = \hbar c/(2.7\, k_B T)$, where c is the sound velocity and $\hbar = 10^{-34}$ (SI) is Planck's constant. $q_{\rm ph}$ is the mean wavevector of thermal phonons. So Eq. 15 is valid if the condition $n < q_{\rm ph}$ is also fulfilled. Equivalently, a departure from a rough behavior is expected when:

(i) $n < 1/3w \approx 0.04/a$

or

(ii) $n < q_{\rm ph} \approx 0.09T/a$ (assuming $c = 400$ m/s).

The first condition is the same as for the crossover of the surface stiffness, and we have seen that this crossover angle decreases slightly as a

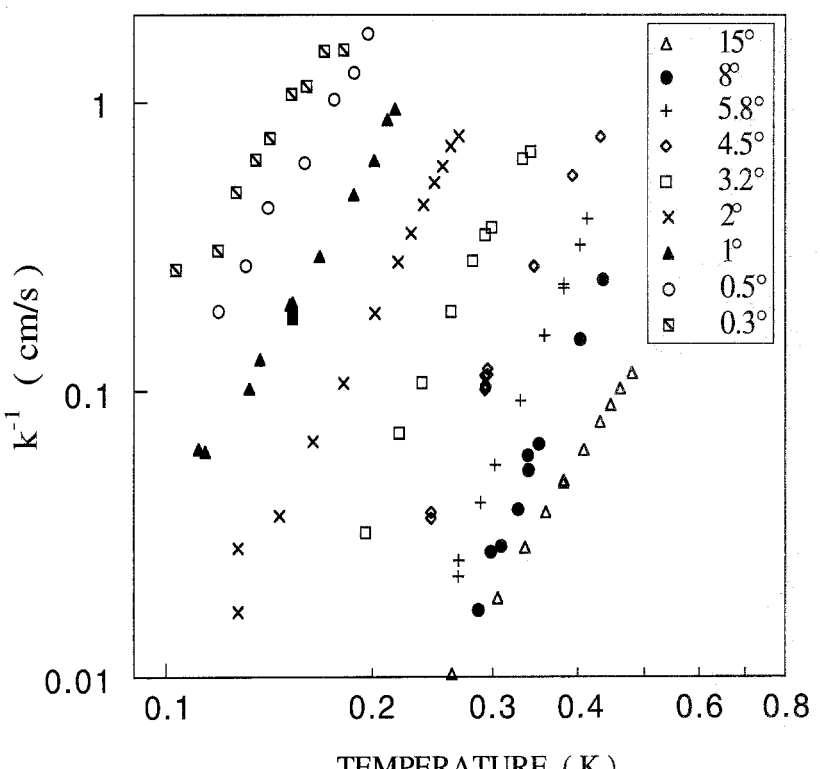

Fig. 13. The growth resistance as a function of temperature, for various values of the orientation. The temperature dependence goes from T^4 at large angle to about T^6 at intermediate angles ($2° < \phi < 8°$) and back to $T^{3.5}$ at the smallest angle 0.3°. This is shown consistent with a change from coherent to incoherent scattering of phonons (see text).

function of T (see Fig. 8). In contrast, the new condition (ii) implies a crossover angle which increases linearly with T. Conditions (i) and (ii) lead to similar crossover angles, and experimental data are needed to find the relevant one.

Let us thus consider our results for orientations close to the c axis ($0.3 < \phi < 15°$). Most of our experimental data are displayed on Fig. 13. The data on this figure correspond to both the longitudinal and the transverse geometry. We have checked that the same results are obtained in both cases. There are two important features to remark on Fig. 13:

(a) The existence of c facets has a strong influence on the growth resistance up to large tilt angles. Indeed, even for $\phi = 8°$, the growth resistance k^{-1} is substantially larger than for a rough orientation. We thus find a crossover angle for the mobility which is much larger than for the surface stiffness.

(b) For intermediate orientations ($2 < \phi < 8°$), the temperature dependence is steeper than for a rough surface. In order to be more precise, one can fit $k^{-1}(T)$ with a power law T^{ν} in the small temperature range available for each orientation. One then finds that ν has a maximum value close to 6 for tilt angles in the range 2–8°. At small angle, ν is smaller ($\nu \approx 3.5$ for $\phi = 0.3°$).

A preliminary observation of similar effects was reported by Andreeva *et al.*[21] We wish here to present a full interpretation of the T and ϕ dependences of the mobility.

In order to understand the mechanism which controls the dissipation, it is easier to use mobility values which are normalized with respect to the mobility of a rough interface k_{rough}. Fig. 14 shows the variation of $k_n = k/k_{\text{rough}}$ as a function of the step density for various temperatures. The crossover is clearly temperature dependent, and the value of the step density n_c at the crossover increases roughly linearly with T. In the frame of the above arguments, the interpretation is clear: in the temperature range of our experiment, the crossover n_c is mainly fixed by the phonon wavelength and not by the step width. This is confirmed by Fig. 15, where k_n is plotted as a function of the normalized step density n/q_{ph}: *all* normalized data now fall on a single curve.

In other words, at low step density, the mobility is reduced because the phonons are scattered independently by the steps. The momentum parallel to the interface is no longer conserved, so that the scattering is incoherent and the dissipation is increased. This is in contrast with the case of a rough interface, which has translational invariance, so that only coherent scattering occurs (i.e., specular reflection).

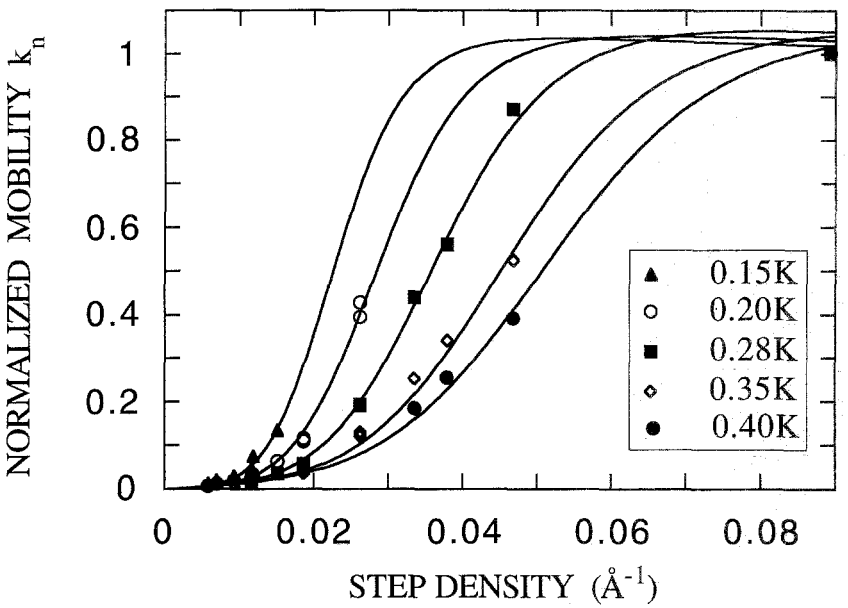

Fig. 14. Normalized mobility as a function of the step density at different temperatures. The corresponding angular range of the data is 1–15°. The crossover from rough to stepped behaviour increases as a function of the temperature. The solid lines are best fits using Eq. 18.

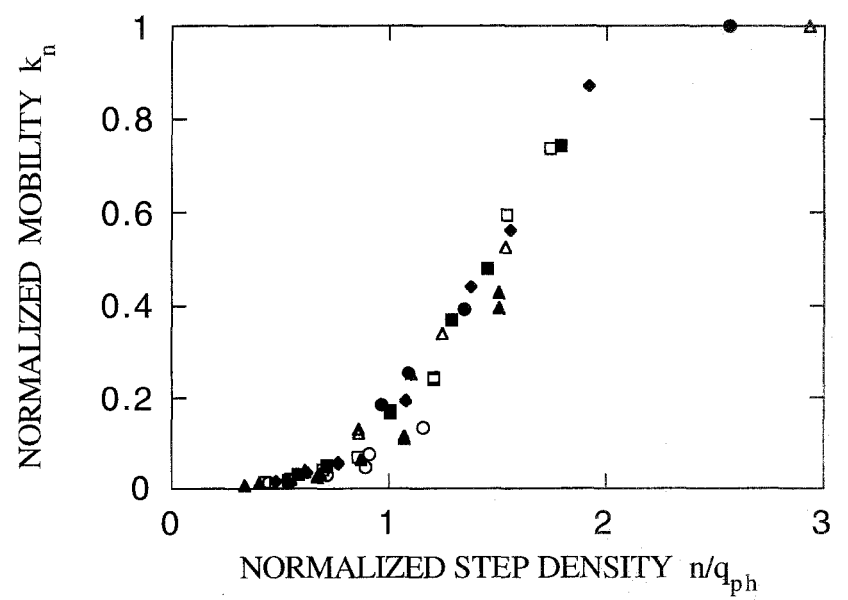

Fig. 15. Normalized mobility as a function of the normalized step density n/q_{ph}. Various symbols correspond to different temperatures. The crossover occurs when $n/q_{\mathrm{ph}} \approx 1.5$.

It is possible to go a little further in the interpretation. NU[28] have derived a semi-empirical relation which describes the variation of the mobility for vicinal surfaces. They propose to write k as follows:

$$k = [nak_s] \times \left[S_{\text{inc}} + \frac{\pi n^3 a^2}{q_{\text{ph}}} \right]^{-1} \times \left[\frac{n^2 + q_{\text{ph}}^2}{q_{\text{ph}}^2} \right] \tag{16}$$

The first bracket is the mobility of a stepped interface, the second one is the inverse of the form factor describing the scattering of phonons (incoherent and coherent parts are written separately). The third bracket accounts for multiple scattering.

The main difficulty in using this expression is due to S_{inc}, for which no expression has been derived. As S_{inc} arises from step fluctuations, a calculation at finite step density should take into account the interactions between steps. Besides the computational difficulty, one lacks a complete theory for step interactions in the crossover. Thus we only know that S_{inc} is equal to one at small n and vanishes at large n. Moreover, the expression for the third bracket has not been rigorously derived. Eventually, Eq. 16 is only valid for a single value of q_{ph}, so that an average on the thermal distribution of phonons is needed.

A precise test of Eq. 16 thus seems difficult. However, we can make a few simple assumptions to check that it describes our observations and that the underlying physics is correct. First we set q_{ph} equal to the mean wavevector of thermal phonons: $q_{\text{ph}} = 2.7 k_B T/\hbar c$, with $c = 400$ m/s, a value intermediate between the velocities of transverse and longitudinal sound in the solid. Secondly, the simplest expression which matches the asymptotic values of S_{inc} is a lorentzian function. We thus assume:

$$S_{\text{inc}} = \frac{1}{1 + b(T)\, n^2} \tag{17}$$

We are thus left with only one adjustable parameter $b(T)$ for each curve $k_n(n)$. We can identify k_{rough} with the limit at large n of k which is $k_s/(a\pi q_{\text{ph}})$. We finally obtain:

$$k_n = \frac{k}{\lim_{n \to \infty} (k)} = [n\pi a^2 q_{\text{ph}}] \times \left[\frac{1}{1 + b(T)\, n^2} + \frac{\pi n^3 a^2}{q_{\text{ph}}} \right]^{-1} \times \left[\frac{n^2 + q_{\text{ph}}^2}{q_{\text{ph}}^2} \right] \tag{18}$$

As can be seen on Fig. 14, the crossover is very well described by Eq. 18. This is a strong argument in favor of the physical mechanism proposed by NU: the decrease of the mobility at small angle is due to

the enhancement of incoherent scattering and the reduction in multiple scattering. We find that the parameter b is a decreasing function of T, so that S_{inc} is an increasing function of T at fixed n. This is consistent with the fact that S_{inc} arises from step fluctuations.

By using the above procedure, we have focused our attention on intermediate and large values of the tilt angle or equivalently of the step density. A different analysis is needed in the small angle limit. Let us thus consider the results obtained at small tilt angle. For a true stepped interface, one is left with the first bracket in Eq. 16: one expects a linear dependence of the mobility as a function of the step density. Moreover, NU have shown that the mobility should vary like T^{-3}. Experimental data are displayed on Fig. 16, for tilt angles ranging from 0.3 to 1°. It can be seen that k reaches its linear asymptotic behavior only at the smallest angle $\phi = 0.3°$. This is confirmed by the temperature variation which we found slightly faster than T^{-3}. An estimate of $k_s = k/na = k/\phi$ can still be obtained by drawing a straight line through the origin and the last two points at 0.3 and 0.5°. At $T = 0.18$ K, we find $k_s \approx 110$ s/cm. This value is quite satisfactory for two reasons. First, NU predicted

$$k_S \approx \frac{\rho_c c a^3}{k_B \theta_D} \left(\frac{\theta_D}{T}\right)^3 \tag{19}$$

where $\theta_D = 26\ K$ is the Debye temperature in the solid.[47] At $T = 0.18$ K, Eq. 19 predicts $k_s = 160$ s/cm, close to our experimental value. Secondly, the extrapolation down to 0.18 K of the mobility of a rough interface yields about 400 s/cm, which is again of the same order of magnitude as k_s. It is a further evidence that one can consider a step as a continuous rough strip which does not feel the lattice potential along the terraces, i.e., a free line with a high density of kinks.

Let us finally come back to the temperature dependence of the growth resistance for intermediate values of the orientation (2–8°). In this case, our temperature range was restricted to 0.2–0.4 K, where a power law close to T^6 was observed. Andreeva *et al.*[21] made similar observations and it was very puzzling because one expected an exponent between 4 and 3, the values for a rough and for a stepped interface. We now understand these results as follows. Consider an interface with a fixed orientation. At low enough temperature, the wavelength of phonons is very large, so that they do not see the structure of the interface. The interface thus looks homogeneous, yielding coherent scattering—i.e., specular reflection—of the phonons. The dissipation is only due to the exchange of momentum perpendicular to the surface. This case is identical to the one of a rough interface, and the dissipation varies like T^4. When the temperature is increased,

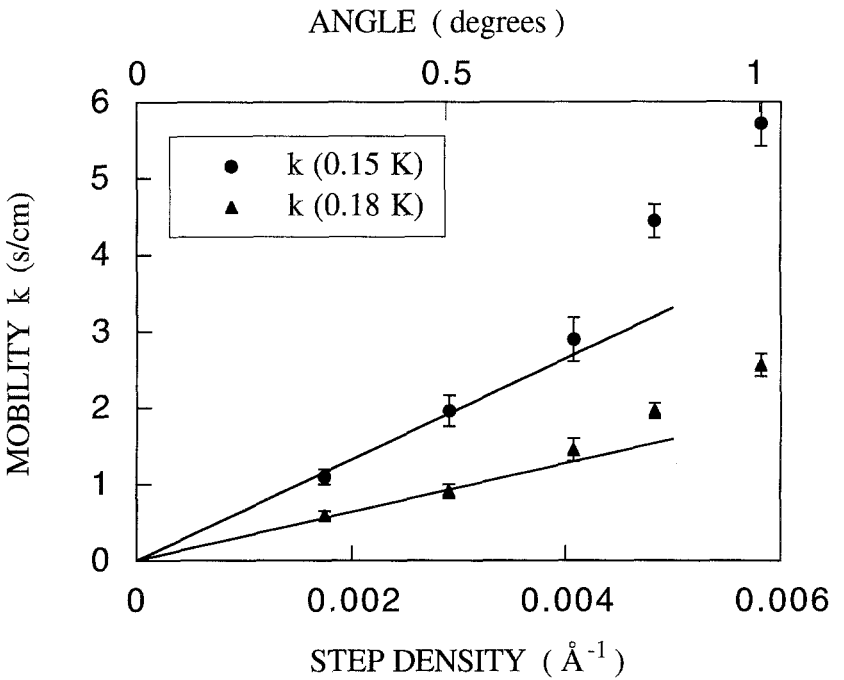

Fig. 16. The mobility as a function of the step density, for small step density (the corresponding angular range is 0.3–1°). The asymptotic behaviour seems linear, as expected for independent steps.

the wavelength of phonons λ_{ph} becomes of the order of the distance d between steps. As phonons see the steps, they can exchange momentum parallel to the interface: incoherent scattering starts. This creates an additional channel for dissipation, yielding a temperature dependence steeper than T^4. If the temperature is further increased, λ_{ph} becomes smaller than d. Some of the incident phonons are reflected on the terraces between the steps; these phonons do not contribute to dissipation since terraces are at rest. The dissipation should then vary rather like T^3, but the precise behavior of k^{-1} in this temperature range also depends on the ratio w/d.

The resulting behavior of k^{-1} is sketched on Fig. 17. For orientations between 2 and 8°, our experimental data lie in the intermediate temperature range, yielding an apparent T^6 variation of k^{-1}. For smaller angles, our results are closer to the asymptotic T^3 behavior.

The variation of k as a function of orientation and temperature can thus be quantitatively understood by carefully considering the scattering of phonons by steps.

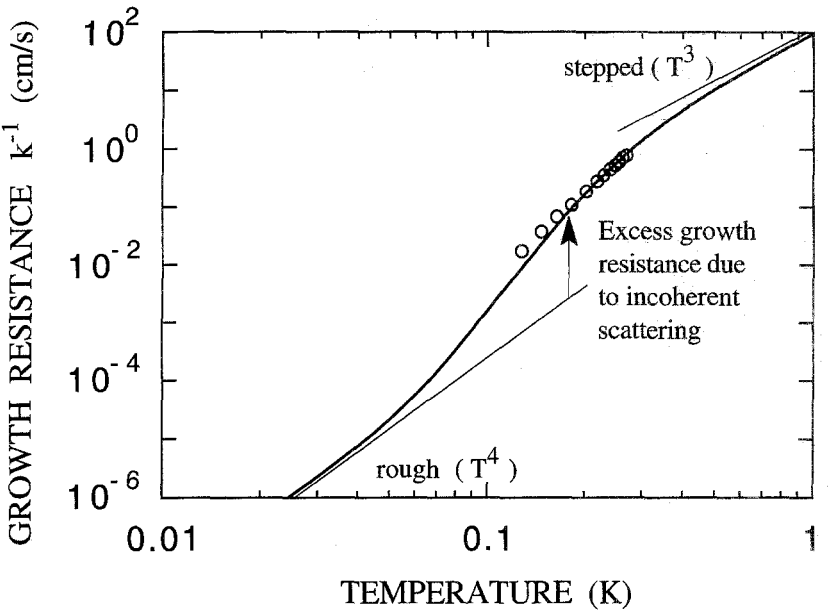

Fig. 17. Sketch of the temperature dependence of the growth resistance, from Eq. 16 ($\phi = 2°$). Circles are experimental data. In the accessible temperature range, the crossover between the rough and stepped regime leads to an apparent T^6 dependence. The stepped regime cannot be reached first because steps are not well separated at $\phi = 2°$, and secondly because dissipation due to rotons is dominant above 0.6 K.

5. CONCLUSION

We hope that this work solves a few controversies and clarifies some of the fundamental properties of vicinal crystal surfaces. We also hope that it triggers new theoretical and experimental efforts. Of particular interest to us would be a calculation of the interaction between steps in a weak coupling situation and when the distance between steps is comparable with their width. One would need to solve a sine-Gordon model for a tilted surface at finite T and with elastic interactions. As for experiments, the most interesting seems to measure the kink energy. One would need to work in the milliKelvin region and the simplest idea seems to measure the shape of c facets. Except if there is a large density of quantum kinks at $T = 0$, the shape of c facets should change from round to hexagonal as T decreases. The kink energy could be extracted from the temperature variation of the facet edge curvature. We also expect helium 3 impurities to adsorb on kinks and change their energy.

ACKNOWLEDGMENTS

We wish to thank P. Nozières for his permanent interest in our work and G. Frossati for crucial help in the cryogenics, as well as all the technicians and engineers in our Department who participated in this difficult experiment, especially J. C. Sutra, J. Kerboriou, J. C. Paindorge, R. Ussiglio, J. Olejnik, D. Le Moal and C. Hermann.

REFERENCES

1. S. Balibar, C. Guthmann, and E. Rolley, *J. Phys. I France* **3**, 1475 (1993).
2. J. D. Weeks and G. H. Gilmer, *Adv. in Chem. Phys.* **40**, 157 (1979).
3. H. van Beijeren and I. Nolden, in "Structure and dynamics of surfaces II," ed. by W. Schommers and P. van Blanckenhagen, Springer 1987.
4. P. Nozières, in "Solids Far From Equilibrium," Lectures at the Beg-Rohu summer school, C. Godrèche ed. (Cambridge University Press, 1991).
5. P. Nozières and F. Gallet, *J. Phys.* (France) **48**, 353 (1987).
6. Strictly speaking, a stepped surface of orientation $\langle n \rangle$ is rough if its height-height correlation function diverges, i.e., above its own roughening temperature T_{Rn}. Below T_{Rn}, steps are registered with respect to the lattice, that is the phenomenon which is considered in Ref. 7. However, if the step density is small, T_{Rn} is very small. Here we only consider temperatures between T_{Rn} and T_{R0}, the roughening temperature of the main terraces. For simplicity we call "stepped" the surfaces whose large anisotropy is due to the existence of well defined steps and terraces, and we restrict the use of "rough" to qualify surfaces at larger tilt angle, whose anisotropy is small because terraces are too narrow to be well defined.
7. J. Lapujoulade, J. Perrau, and A. Kora, *Surf. Sci.* **129**, 59 (1983); J. Villain, D. R. Grempel, and J. Lapujoulade, *J. Phys. F* **15**, 804 (1985); J. Lapujoulade, in "Interaction of atoms and molecules with solid surfaces", ed. by V. Bortolani *et al.* p. 381 (Plenum, 1990).
8. C. Jayaprakash, W. F. Saam, and S. Teitel, *Phys. Rev. Lett.* **50**, 2017 (1983); C. Rottman and M. Wortis, *Phys. Rev. B* **29**, 328 (1984).
9. N. C. Bartelt, T. L. Einstein, and E. Williams, *Surf. Sci. Lett.* **240**, 591 (1990); E. Williams and N. C. Bartelt, *Science* **251**, 393 (1991).
10. M. Kardar and D. R. Nelson, *Phys. Rev. Lett.* **55**, 1157 (1985).
11. M. Uwaha, *J. Low Temp. Phys.* **77**, 165 (1989); M. Uwaha, *J. Phys.* (France) **51**, 2743 (1990).
12. H. van Beijeren, private communication.
13. C. Rottman, M. Wortis, J. C. Heyraud, and J. J. Métois, *Phys. Rev. Lett.* **52**, 1009 (1984); J. J. Saenz and N. Garcia, *Surf. Sci.* **155**, 24 (1985).
14. J. J. Métois and J. C. Heyraud, *Surf. Sci.* **180**, 647 (1987).
15. F. Gallet, Ph.D. thesis, unpublished, Paris (1986); Y. Carmi, S. G. Lipson, and E. Polturak, *Phys. Rev. B* **36**, 1894 (1987). New results have very recently been obtained on helium 4 crystals by A. V. Babkin (private communication) with an improved interferometric technique.
16. X. S. Wang, J. L. Goldberg, N. C. Bartelt, T. L. Einstein, and E. Williams, *Phys. Rev. Lett.* **65**, 2430 (1990).
17. C. Alfonso, J. M. Bermond, J. C. Heyraud, and J. J. Metois, *Surf. Sci.* **262**, 371 (1992).
18. S. Balibar, C. Guthmann, and E. Rolley, *Surf. Sci.* **283**, 290 (1993).
19. J. Frohn, M. Giesen, M. Poengsen, J. F. Wolf, and H. Ibach, *Phys. Rev. Lett.* **67**, 3543 (1991).
20. K. O. Keshishev, A. Ya. Parshin, and A. V. Babkin, *Pis'ma Zh. Eksp. Teor. Fiz.* **30**, 63 (1979) [*Sov. Phys. JETP Lett.* **30**, 56 (1979)].

21. O. A. Andreeva and K. O. Keshishev, *Pis'ma Zh. Eksp. Teor. Fiz.* **46**, 160 (1987) [*Sov. Phys. JETP Lett.* **46**, 200 (1987)]; O. A. Andreeva, K. O. Keshishev, and S. Yu. Osip'yan, *Pis'ma Zh. Eksp. Teor. Fiz.* **49**, 661 (1989) [Sov. Phys. JETP Lett. **49**, 759 (1989)]; O. A. Andreeva, K. O. Keshishev, A. V. Kogan, and A. N. Marchenkov, *Europhysics Letters* **19**, 683 (1992).
22. A. F. Andreev, in *Excitations in 2D and 3D Quantum Fluids*, ed. by A. F. G. Wyatt and H. J. Lauter (Plenum, New York 1991), p. 397; K. O. Keshishev and O. Andreeva, ibid. p. 387.
23. E. Rolley, E. Chevalier, C. Guthmann, and S. Balibar, *Phys. Rev. Lett.* **72**, 872 (1994).
24. V. I. Marchenko and A. Ya. Parshin, *Zh. Eksp. Teor. Fiz.* **79**, 257 (1980) [*Sov. Phys. JETP* **52**, 129 (1980)].
25. C. Jayaprakash, C. Rottman, and W. F. Saam, *Phys. Rev. B* **30**, 6549 (1984).
26. Y. Akutsu, N. Akutsu, and T. Yamamoto, *Phys. Rev. Lett.* **61**, 424 (1988). Their prediction for the entropic interaction in terms of the step energy can also be obtained from the work of Bartelt, Williams *et al.*[9] who used the work of C. Jayaprakash *et al.*[25] However, the hopping matrix element in Ref. 25 should be doubled (W. F. Saam, private communication, sept. 93). Hence the amplitude of the entropic interaction is also too small by a factor 2 in Ref. 9.
27. E. Rolley, S. Balibar, C. Guthmann, and P. Nozières, *Jyväskylä meeting* (Finland, june 1994) to appear in *Physica B* **210** (May 1995).
28. P. Nozières and M. Uwaha, *J. Physique* **48**, 389 (1987).
29. Type Ta2 infrared filters purchased from MTO, Massy, France.
30. The ^{3}He concentration is 4×10^{-10} (US Bureau of Mines certificate #(806) 376 2367 FTS 735–1367).
31. P. E. Wolf, F. Gallet, S. Balibar, E. Rolley, and P. Nozières, *J. Physique* (France) **46**, 1987 (1985).
32. C. Guthmann, S. Balibar, E. Chevalier, E. Rolley, and J. C. Sutra-Fourcade, *Rev. Sci. Inst.* **65**, 273 (1994).
33. P. R. Roach, J. B. Ketterson, and M. Kuchnir, *Rev. Sci. Inst.* **43**, 898 (1972).
34. C. L. Wang and G. Agnolet, *J. Low Temp. Phys.* **89**, 759 (1992); *Phys. Rev. Lett.* **69**, 2102 (1992).
35. A. F. Andreev and A. Ya. Parshin, *Zh. Eksp. Teor. Fiz.* **75**, 1511 (1978) [*Sov. Phys. JETP* **48**, 763 (1978)].
36. F. Gallet, S. Balibar, and E. Rolley, *J. Physique* (France) **48**, 369 (1987).
37. F. Pederiva, A. Ferrante, S. Fantoni, and L. Reatto, *Phys. Rev. Lett.* **72**, 2589 (1994).
38. A. V. Babkin, D. B. Kopeliovitch, and A. Ya. Parshin, *Zh. Eksp. Teor. Fiz.* **89**, 2288, (1985) [*Sov. Phys. JETP* **62**, 1322 (1985)].
39. J. Treiner, *J. Low Temp. Phys.* **92**, 1 (1993).
40. E. Varoquaux, G. G. Ihas, O. Avenel, and R. Aarts, *Phys. Rev. Lett.* **70**, 2114 (1993).
41. D. O. Edwards, M. S. Petersen, and H. Baddar, in *Excitations in 2D and 3D Quantum Fluids*, ed., by A. F. G. Wyatt and H. J. Lauter (Plenum, New York 1991), p. 361.
42. H. J. Maris and T. E. Huber, *J. Low Temp.* **48**, 99 (1982).
43. P. Nozières, private communication.
44. B. Castaing, S. Balibar, and C. Laroche, *J. Physique* (France) **41**, 897 (1980); J. Bodensohn, K. Nicolai, and P. Leiderer, *Z. Phys. B* **64**, 55 (1986).
45. R. M. Bowley and D. O. Edwards, *J. Physique* (France) **44**, 723 (1983).
46. A. A. Golub and S. V. Svatko, *Fiz. Nisk. Temp.* **6**, 957 (1980) [*Sov. J. Low Temp. Phys.* **6**, 465 (1980)].
47. D. S. Greywall, *Phys. Rev. B* **16**, 5127 (1977).